Bioresource Technology 150 (2013) 98–105

Contents lists available at ScienceDirect

Bioresource Technology

journal homepage: www.elsevier.com/locate/biortech

Chemical and morphological changes in hydrochars derived from microcrystalline cellulose and investigated by chromatographic, spectroscopic and adsorption techniques

Mamadou Diakité [a,*], Andrea Paul [b], Christian Jäger [b], Judith Pielert [c], Jan Mumme [a]

[a] Leibniz Institute for Agricultural Engineering Potsdam-Bornim e.V., Max-Eyth-Allee 100, 14469 Potsdam, Germany
[b] BAM, Federal Institute for Materials Research and Testing, Richard-Willstätter-Straße 11, 12489 Berlin, Germany
[c] Department of Soil Science, Technische Universität Berlin, Ernst-Reuter-Platz 1, 10587 Berlin, Germany

HIGHLIGHTS

- Hydrochars from MCC are characterized by a multi method approach.
- Between 230–270 °C and 2–10 h, the carbon content changes were very weak.
- FT-IR and NMR yield detailed information on the functional groups in hydrochars.
- Surface area and pore volume was highest at 230 °C, and aromaticity at 270 °C.

ARTICLE INFO

Article history:
Received 1 August 2013
Received in revised form 26 September 2013
Accepted 28 September 2013
Available online 8 October 2013

Keywords:
Hydrothermal carbonization
Hydrochar
Microcrystalline cellulose
NMR-spectroscopy
ATR-FTIR-spectroscopy

ABSTRACT

Hydrothermal carbonization (HTC) can be used for converting the biomass into a carbon-rich material, whose application as a fuel requires higher heating value, whereas soil amendment needs stable carbon. This work was focused on the characterization of hydrochars derived from microcrystalline cellulose. The chars were investigated using elemental analysis, Brunauer–Emmett–Teller technique, nuclear magnetic resonance spectroscopy, Raman, Fourier transform infrared, and electron spin resonance spectroscopy. Severity in temperature between 230 and 270 °C with reaction times between 2 and 10 h only affect the carbon content moderately. The results show that aromatization of HTC chars correlates well with temperature, which was further supported by the increase of organic radicals with decreasing g values at higher temperatures. Based on these results, the energetic use of chars favors mild HTC ($T < 230$ °C and $t \leqslant 6$ h), while the soil amendement favors serve conditions ($T \geqslant 230$ °C, and $t > 6$ h).

© 2013 Elsevier Ltd. All rights reserved.

1. Introduction

In the case of global warming, pyrolysed biomass, well-known as biochar, is vividly discussed as an option to remedy the CO_2 accumulation in the atmosphere. Furthermore, the production of biochar is considered as a promising way to valorize various organic wastes, such as municipal, industrial, agricultural, and forestry waste. Besides the beneficiation of climate change, biochar offers other potential applications including soil improvement (Lehmann and Joseph, 2009), chemical filter for the degradation of organic pollutants (Weiner et al., 2013), and alternative solid fuel (Reza et al., 2013). However, the practical implementation of biochar is still questioned for its economic viability and possible toxic effects for the environment (Reddy, 2010). Whereas conventional gasification, pyrolysis, and torrefaction are established thermochemical methods for biomass valorization, HTC is a relative new process. The specific advantage of HTC over the other thermochemical treatments, is the ability to use wet feedstocks. However, the process takes place under high pressure (2–5 MPa), which can be a limiting factor in plant design and system efficiency. HTC is a method for thermochemical treatment of various organic wastes for producing chars, which may be defined as hydrochars. The physical and chemical characteristics of hydrochars differ for a wide range of applications such as soil application, energy purpose, sorption of toxic compounds, purification, and catalysis (Goto et al., 2004; Wang et al., 2011).

For soil application, hydrochars are considered to improve soil quality, to increase crop yields, and to sequestrate carbon (Goto et al., 2004; Reddy, 2010). Hence, for soil application, hydrochar must be designed specially with distinct physical and chemical properties such as high surface area, low bulk density, neutral pH

---

* Corresponding author. Tel.: +49 331 5699 900; fax: +49 331 5699 849.
E-mail address: mdiakite@atb-potsdam.de (M. Diakité).

0960-8524/$ - see front matter © 2013 Elsevier Ltd. All rights reserved.
http://dx.doi.org/10.1016/j.biortech.2013.09.129

(for improving sorption capacity of nutrients), high aromaticity (as an indicator of the carbon stability in soil), and absence of toxic compounds. These stated properties are greatly influenced by both the feedstock as well as process conditions (Day et al., 2005; Sevilla and Fuertes, 2009). Recently, Becker et al. (2013), showed that the amount of volatile organic compounds (VOCs) in hydrochar can be correlated with the phenolic compounds and the process temperature. In fact, the amount of VOCs and phenolic compounds increases proportionally with process temperature, which is also known as phytotoxic effect. Meanwhile, the degree of condensation in carbonaceous material depends on the temperature and reaction time of the thermal treatment. Therefore, the optimal process conditions must be identified, where the physical and chemical properties of hydrochars are ideal for the application in soils along with lower VOC content.

The mechanism of HTC includes the dehydration of the carbohydrate into furan-like molecules (furfural aldehyde and/or 5-(hydroxymethyl)-2-furaldehyde), subsequent polymerization (condensation), and decarbonization (Sevilla and Fuertes, 2009; Titirici et al., 2008). Input materials and process conditions affect the chemical properties of hydrochars such as elemental composition (Mumme et al., 2011; Sevilla and Fuertes, 2009). This also applies to the physical parameter such as specific surface area, specific pore volume, and pore size distribution. For potential applications like chemical absorbent, and/or soil improvement, the specific surface area of hydrochar is an important physical property, which is affected by the process conditions such as temperature and pH (Sevilla and Fuertes, 2009; Mumme et al., 2011). The pore volume can be divided into macro-and micro-pores. For example, micropores contribute most to the surface area of biochar and to a higher adsorptive capacities (Rouquerol et al., 1999), while macropores may provide a suitable habitat for microorganisms in the soil (Lehmann and Joseph, 2009).

The hydrothermal treatment of biomass has been described by various authors. For process engineering, the chemical mechanism of the HTC has been investigated by Funke and Ziegler (2010), and the reaction kinetics by Reza et al. (2013). Stemann gives an overview of the characteristic properties of the resulting liquid phase during the hydrothermal carbonization of lignocellulosic biomass in Stemann et al. (2013). A comparative review of the wet (HTC) and dry pyrolysis was given by Libra et al. (2011). From the viewpoint of process engineering, energy efficiency and product quality require sufficient insight of the thermochemical conversion process as they are a prerequisite for effective reactor and process design. The emphasis of this work was therefore answer the question, to which extent temperature, pH, and time influence on the physicochemical properties of hydrochar, and how these changes can be characterized efficiently.

For this purpose, the physico-chemical properties of different hydrochars derived from cellulose were studied under the variation of process temperature, initial pH, and reaction time based on a Box–Behnken partial factorial design. Cellulose is one of the major constituents of all types of natural organic matter used in hydrochar production. Therefore, and because of the high homogeneity of the material, cellulose derived hydrochars were prepared as a model compound. Special emphasis was placed on the char's elemental composition, such as carbon, hydrogen, nitrogen, and sulphur (CHNS), the final pH of the char-liquor-suspension, and Brunauer, Emmett, and Teller (BET) surface area. In addition, selected samples were characterized by nuclear magnetic resonance (NMR), electron spin resonance (ESR), Fourier-transformed infrared (FTIR), and Raman spectroscopy to identify changes on a molecular level. Based on the spectroscopic data, furthermore, a comparison to previous studies is possible as those methods are widely used to identify the molecular structures of various products in biochar production (Ingram et al., 1954; Titirici et al., 2011).

2. Methods

2.1. Experimental procedure

The industrial microcrystalline cellulose (MCC), Avicel PH 101 (Sigma–Aldrich, Switzerland), was used as the sole feedstock in this study. Avicel PH 101 is a microcrystalline, powdery material with an average particle size of 50 μm and a bulk density of 0.28 g/cm^3. The experiments were carried out in a 1 L stirred pressure reactor using distilled water as a process medium. The reactor's initial dry matter concentration of Avicel was 97 g/L. Process temperatures were 190, 230, and 270 °C, while reaction times were 2, 6, and 10 h and pH values maintained at 3, 5, and 7, by applying citric acid. The working pressure range was between 1.7 MPa (at 190 °C) and 2.9 MPa (at 270 °C). The statistical software "Design Expert" was used to plan and evaluate the experimental work, using a Box–Behnken partial factorial design. This reduced the number of trials from 27 (3^3) to 15.

2.2. Characterization of physicochemical properties

The specific surface area was determined based on nitrogen adsorption and the BET method. The sample CE-10 (at 190 °C) hat to be carefully pestled to enable filling into sample cells. The samples were degassed under vacuum at 20 °C until pressure increase was ⩽10 micron per minute. This required degassing time of hydrochars between 53–72 (sample CE-10), 39–49 (sample CE-09), and 19–33 h (sample CE-12). All surface and porosity analyses were made with a Autosorb-1 (Quantachrome) using nitrogen as adsorbate. The adsorption and desorption isotherms were evaluated a 77 K. In the relative pressure range P/P_0 of 0.05–0.3 the specific surface area of the chars was quantified with the BET adsorption method (use of BET equation ISO 9277). Micropores were determined by Dubinin–Radushkevich (DR) adsorption method (DIN 66135-3) in a relative pressure range of 0.00,004–0.08. The analysis of mesopores was determined in a relative pressure range of 0.99–0.3 according to Barrett, Joyner and Halenda (BJH) desorption method (DIN 66134).

To investigate the influence of the process setting on the hydrochars' microscopic structure, the surface morphology of the hydrochars was studied using the Hitachi scanning electron microscope (SEM) S-2700. The dried (105 °C) sample material was mounted on the sample holder and sputtered with about 25 nm of gold (to avoid electrical charging of samples). The SEM images were made at the ZELMI at the technical university to Berlin.

2.2.1. The ultimate analysis

The ultimate analysis was obtained by using carbon, hydrogen, nitrogen, and sulphur (CHNS) analyzer (Elementar Analysensysteme Hanau, Germany). Each sample was analyzed three times, and the oxygen composition calculated by the difference method ($O\% = 100 - (C\% + H\% + N\% + S\%)$). Dry matter (DM) was determined by treating feedstock at 105 °C for 24 h and the heat of combustion was calculated using the correlation of Boie (1953). The gel-based probe SenTix41 (WTW, Weilheim, Germany) was used to determine the pH of the liquid phase, and a Fisons GC-FID 8000 from Thermo Fischer Scientific (Italy), equipped with a PERMABOND FFAP capillary column to determine the concentration of volatile fatty acids.

2.2.2. Nuclear magnetic resonance (NMR) spectroscopy

Spectroscopic characterization was in general performed on powdered, dry samples processed over 6 h at pH 5 without any further treatment. *Solid state ^{13}C cross polarization magic angle spinning*

(CP/MAS)-NMR experiments were performed on a Bruker Avance 400 spectrometer (9.4 T) operating at 100.4 MHz for ^{13}C and 400.1 MHz for ^{1}H NMR. All experiments were carried out at room temperature using a 4 mm MAS with a frequency of 12.5 kHz. All spectra were acquired using a 90° ^{1}H pulse length of 3.2 μs, a contact time of 1 ms and a repetition time of 3 s. The ^{13}C spin lock field was held constant while the ^{1}H spin lock field was ramped down to 50% of its initial value. 2048 scans were accumulated and high power proton decoupling was carried out during data acquisition with a 15° two pulse phase modulation (TPPM) sequence (Bennett et al., 1995). Data processing was performed with the software TopSpin. ^{13}C chemical shifts (δ) are reported relative to Tetramethylsilane (TMS) using the COOH resonance of glycine at $\delta = 176.45$ ppm as a secondary solid standard.

2.2.3. Attenuated total reflection-Fourier transform infrared (ATR-FTIR) spectroscopy

Attenuated total reflection-Fourier transform infrared (ATR-FTIR) spectroscopy was used to obtain information on the molecular vibrations of the hydrochar. The spectra were measured with an IFS66v FTIR spectrometer (Bruker) using a diamond ATR accessory (Golden Gate, Specac) with a resolution of 2 cm^{-1} from 4000 to 600 cm^{-1} over 100 scans.

2.2.4. Raman scattering (Raman spectroscopy)

Raman scattering (Raman spectroscopy) was investigated with a DILOR XY laser Raman spectrometer based on a nitrogen cooled Charge Coupled Device camera multi-channel detector with a back scattering geometry by micro Raman technique (BH2-Olympus microscope 50×). All spectra were recorded at room temperature with the 514.5 nm line of a cw argon ion laser (ILA120-1, CZ Jena) for excitation. In general, 30 accumulations were recorded with an integration time of 10 s at a resolution of 1 cm^{-1}. Samples were pressed into tablets before the measurement to achieve an even surface. To avoid chemical changes by laser burning, the laser power was reduced to 0.25 mW and all samples were checked by a microscope prior analysis.

2.2.5. Electron spin resonance (ESR) spectroscopy

Electron spin resonance (ESR) spectroscopy was used to provide information on both the number and the nature of organic radicals in the char. CW X-band ESR-spectra were recorded using an ESR spectrometer (MiniScope MS 300, Magnettech GmbH, Berlin, Germany) in quartz glass sample tubes with an inner diameter of 3 mm at 291 K. All spectra were measured at 2 mW microwave power and a field modulation amplitude of 0.125 mT. An internal manganese standard (Mn^{2+} in ZnS, Magnettech GmbH, Berlin, Germany) was used to determine the *g* values. Spin concentrations were calculated using R,R-diphenyl-picryl-hydrazyl (DPPH) dissolved in toluene as a reference (Yordanov and Christova, 1997). Absolute radical concentrations were calculated after double integration of spectra and quantitative comparison to the DPPH spectrum.

3. Results and discussion

3.1. Structural changes by BET, SEM and NMR

The physical changes induced by the thermal treatment with respect to the pore structure and specific surface area were investigated by BET, DR, and BJH and results are presented in Table 1. The BET surface area was found 2.816–27.800 m^{2} g^{-1} and the maximum was at the HTC temperature of 230 °C. This is rather low when compared with the typical surface area of pyrogenic charcoal (120–460 m^{2}/g, depending on input material and process conditions) (Day et al., 2005). The solid product obtained at 190 °C showed macro-scale particles with a relatively smooth surface (see Fig. S1A), and a hard consistency like plasticized synthetic material. This behavior was previously reported by Sevilla and Fuertes (2009) and can be explained by the fact that temperatures at or above 190 °C enhance the crystallinity of MCC (Sandermann and Augustin, 1964). The structure of the cellulose is affected by the crystallinity, the degree of crystalline arrangements in its macromolecules. The crystallinity of cellulose is often used to describe a thermal or chemical treatment affect in its structure (Park et al., 2010). Following Sandermann and Augustin (1964), the thermal degradation of lignocellulose starts at temperatures of 240–340 °C depending on process conditions. According to this study, the hydrothermal destruction of MCC starts between 190 and 230 °C. This is in accordance with other groups hypothesizing an onset of HTC of MCC at 220–230 °C (Sevilla and Fuertes, 2009). Temperatures above 200 °C left an even crusty surface probably due to the formation of gas (Sandermann and Augustin, 1964). This behavior was also found in the present study. By means of SEM analysis, it can be shown that 230 and 270 °C yield porous surface with nano-size particles (Fig. S1B and C), whereas at 190 °C, the product (Fig. S1A) surface is similar to the original MCC. Table 1 also presents a quantitative analysis of surface area and pore volume for different HTC products. At 230 °C, the specific volume of micropores and mesopores are 0.008 and 0.11 cm^{3} g^{-1}, respectively, whereas 270 °C shows only 0.002 and 0.02 cm^{3} g^{-1}, respectively. This might be a result of the accelerated degradation of crystallized structure, when temperature increases above 230 °C (Sandermann and Augustin, 1964).

The spectra of ^{13}C CP/MAS-NMR measurements of pristine MCC and MCC treated at 190 °C are also shown in Fig. S2. The spectrum of the pristine MCC with the signals of 60–110 ppm is characteristic for a semi-crystalline cellulose-I, a mixture of cellulose Iα (triclinic), and Iβ (monoclinic). As shown in Fig. S2, the solid state ^{13}C CP/MAS-NMR spectroscopy considers both crystalline and non-crystalline (amorphous) cellulose regions. The main difference between the spectra of the original and the MCC treated at 190 °C, is the height of the crystalline (c^{1}) and amorphous (a^{1}) peak. While the amorphous peak at 190 °C decreases, the thermal treatment of MCC leads to a significant increase of the crystalline peak. Since, there is no significant new signal, this effect can be explained by a possible modification of the molecular structure of cellulose by the influence of water, and not only by the preferential conversion of the cellulose in the amorphous regions. So, hydrochars formed at 230 °C exhibit a higher surface area, and higher number of micro- and mesopores than hydrochar treated at 190, or 270 °C. It can be concluded that despite the relatively small change of carbon content at 230 (max 69.94%), and 270 °C (max 75.27%) (Table 2), considerable morphologic changes occur during HTC at 270 °C. The finding is similar with Sandermann and Augustin (1964), who suggested that the degradation of structure of MCC proceeds at temperatures over 240 °C. For the technical applications of hydrochar where the surface area and the pore structure plays an important role (such as sorption process), the BET technique could be very helpful in the selection of optimal process conditions.

3.2. Influence of temperature and reaction time

The char yield (based on the amount of MCC) was 72.43–89.73% (at 190 °C), 46.30–48.50% (at 230 °C), and 44.50–46.60% (at 270 °C), where the higher the residence time, the lower the char yield. Table 2 shows the influence of reaction conditions (temperature, reaction time, start pH) on HTC, as well as the char's elemental compositions and the final pH of the reactor slurry. The impact of the process settings on the carbonization level is also shown in Fig. 1. As expected, the products formed at 230 and

Table 1
Specific surface area and porosity of hydrochars produced at 190 °C/pH5/10 h, 230 °C/pH5/6 h, and 270 °C/pH5/10 h.

Sample	T (°C)	W^a (g)	W^b (g)	Time[f] (h)	Surface area ($m^2 g^{-1}$)			Volume ($cm^3 g^{-1}$)			D^e (nm)
					BET	DR[c]	BJH[d]	BET	DR[c]	BJH[d]	
CE-10	190	0.9361	0.8824	72	2.816	2.068	2.665	0.0166	0.0007	0.009	2.574
CE-10	190	0.9378	0.8843	53	2.987	2.200	3.090	0.0150	0.0008	0.008	2.751
CE-10	190	1.4455	1.3996	59	3.290	1.884	3.569	0.01,493	0.0007	0.008	2.498
CE-09	230	0.5832	0.5563	39	27.970	23.540	18.780	0.3120	0.0084	0.068	2.591
CE-09	230	0.6391	0.6099	49	26.570	22.320	19.459	0.4623	0.0080	0.157	2.550
CE-09	230	0.4559	0.4357	41	28.800	22.980	22.200	0.3333	0.0082	0.101	2.590
CE-12	270	0.5221	0.4944	23	8.074	5.807	7.587	0.0483	0.0021	0.020	2.726
CE-12	270	0.6201	0.5898	33	7.679	5.792	6.468	0.0460	0.0021	0.018	2.728
CE-12	270	0.4027	0.3807	19	9.003	5.795	9.218	0.0603	0.0021	0.025	2.719

[a,b] Sample weight before and after the degassing.
[c] Micropore.
[d] Mesopore.
[e] Average particle diameter.
[f] Degassing time.

Table 2
Experimental conditions, elemental composition, heating value of HTC chars derived from MCC, and the carboxylic acids in the HTC liquid phase.

Sample	Process conditions					Elemental composition (% AFDW)[a]					HV[e]	Liquid phase (g/l)[h]	
	T (°C)	t_R (h)	pH1[d]	pH2[d]	p (MPa)	C	H	O[b]	S	N	(MJ/kg)	A[f]	P[g]
MCC[c]	–	–	6.5	6.5	–	43.67	6.70	49.55	0.02	0.06	15.83		
CE-01	190	2	5	3.26	1.1	42.52	7.25	47.44	0.03	0.08	15.87	0.080	<0.02
CE-03	190	6	3	2.64	1.1	43.31	6.80	49.81	0.02	0.06	15.77	0.250	<0.02
CE-10	190	10	5	2.58	1.1	45.02	6.79	48.03	0.12	0.03	16.56	0.280	0.020
CE-13	190	6	7	3.20	1.1	42.83	7.22	49.87	0.02	0.07	15.98	0.160	<0.02
CE-05	230	2	3	2.33	2.6	68.56	4.26	27.05	0.07	0.06	24.93	0.890	0.080
CE-08	230	2	7	2.48	2.6	63.77	6.27	29.80	0.05	0.10	24.81	1.050	0.070
CE-09	230	6	5	2.46	2.6	67.08	4.28	28.36	0.24	0.04	24.28	1.050	0.080
CE-15	230	6	5	2.77	2.6	68.96	4.78	26.09	0.12	0.05	26.68	0.730	0.060
CE-02	230	10	3	2.61	2.6	69.45	3.99	26.43	0.07	0.06	25.06	1.160	0.090
CE-07	230	10	7	2.61	2.6	68.40	4.87	26.57	0.06	0.10	25.50	1.260	0.090
CE-14	270	2	5	2.78	5.6	71.16	3.86	24.68	0.26	0.05	25.70	1.350	0.120
CE-04	270	6	3	2.65	5.6	75.27	2.65	21.92	0.09	0.08	26.38	1.440	0.140
CE-06	270	6	7	2.78	5.4	72.53	3.91	23.41	0.06	0.08	26.42	1.850	0.160
CE-12	270	10	5	2.78	5.6	72.74	2.84	24.30	0.06	0.06	25.38	1.600	0.160

[a] AFDW, ash-free dry weight.
[b] Calculated by subtracting the percentage of C, H, N and S from 100%.
[c] MCC, microcrystalline cellulose.
[d] pH1 = before HTC; pH2 = after HTC.
[e] Heating value.
[f] Concentration of acetic acid in the liquid phase.
[g] Concentration of propionic acid in the liquid phase.
[h] Concentration of butyl acid, iso butyl acid, valeric acid, and iso valeric acid: <0.02 g/l.

270 °C are carbon-rich and can, therefore, be classified as hydrochars. At a reaction time of 6 h, the average carbon content of 69.94% and 75.27% was found, respectively at 230 and 270 °C. At 190 °C only a small change in the carbon content (from 43.67% to 45.02%) could be observed even at the prolonged reaction time of 10 h. The result agrees with literature for low temperature treatment (⩽200 °C of MCC) (Sevilla and Fuertes, 2009). Around this temperature, water and organic products such as short chains carbohydrates are formed (Sandermann and Augustin, 1964). Moreover, the hydrolytic splitting begins in the amorphous regions of cellulose so that the degree of crystallization increases with increasing temperature. Hoeckman et al. (2011) reported that temperatures ⩽200 °C could, in fact, lead into carbonization of cellulose, when a longer reaction time is applied. According to the present study, at 190 °C the required reaction time must exceed 10 h for any noticeable carbonization. However, the carbonization behavior between 190 and 270 °C is important for the design of the carbonization kinetics. To obtain a more comprehensive view of the HTC of MCC, experimental data from Sevilla and Fuertes (2009) were including into the interpretation of the results from the present study (see Fig. 2). Based on the slope of the carbonization curve, three different areas can be identified: the first, second, and third area. Hydrolysis, a relatively rapid process, and crystallization, rather slower process, take place at temperatures below 200 °C (Sandermann and Augustin, 1964). The reaction times below 6 h results no increase in carbon content. Temperatures of 230–250 °C lead to a substantial increase of carbon content in hydrochars of MCC from 43.67% (pristine cellulose) to 63.77–69.94%, might be because of dehydration. The hydrothermal carbonization at 270 °C contribute to condense the carbonaceous structure, a slower process that leads towards a moderate increase in carbon content (cf. Table 2). For a precise separation of the areas of faster and slower carbonization, the kinetic model for the hydrothermal carbonization of loblolly pine was evaluated at temperatures of 200, 230, and 270 °C (Reza et al., 2013). The results show a rate constant (k_2) of the HTC of 0.0022 at 200 °C, 0.0085 at 230 °C, and 0.0200 at 260 °C, confirming that there are areas of slower and faster carbonization. At 230 °C, reaction times of 2, 6, and 10 h showed a weak impact on the carbon content (67.08–69.94%) (cf. Table 2). This behavior, also observed by Sevilla and Fuertes (2009) at 250 °C, indicates a faster carbonization area of MCC. Similar effects were reported by Hoeckman et al. (2011), on

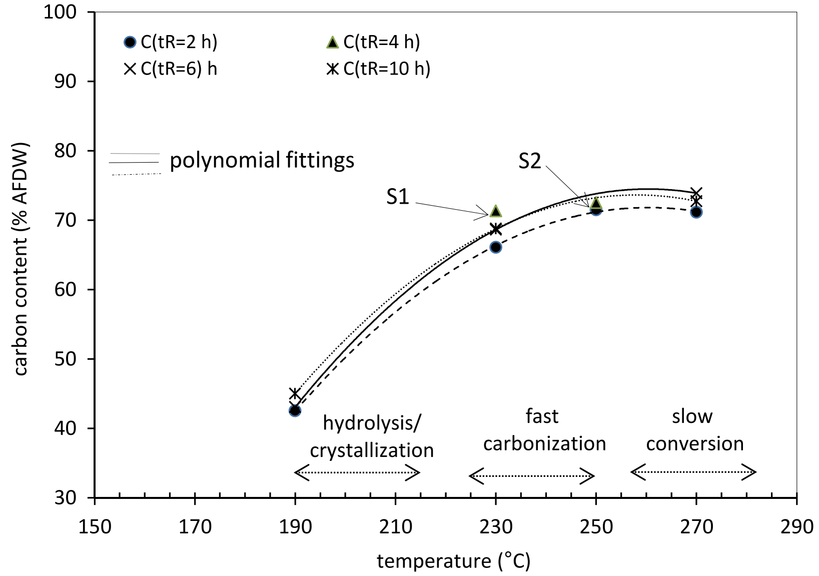

Fig. 1. Temperature and reaction time impact on the carbon content of HTC chars (S1, S2, and S3 are obtained from Sevilla and Fuertes (2009).

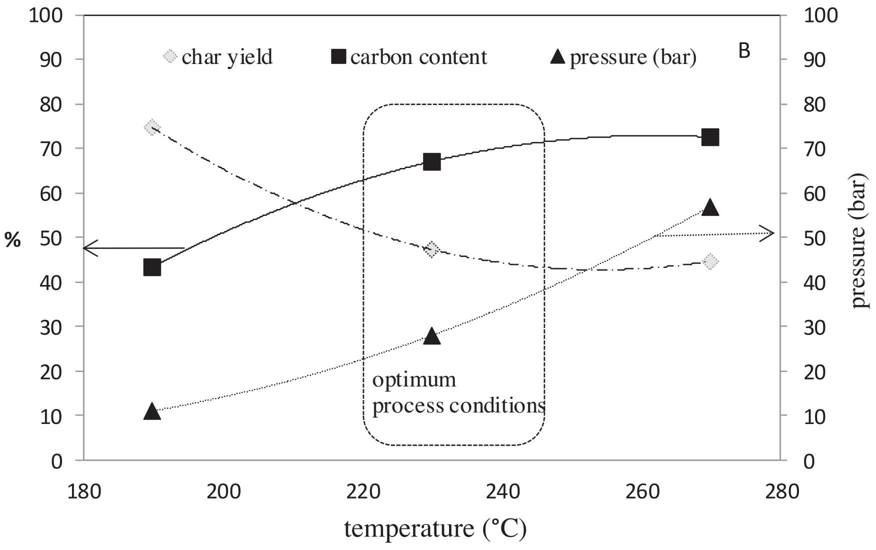

Fig. 2. The impact of temperature and reaction time of 6 h on char yield (dry mass basis), carbon content and reaction pressure.

a HTC of Tahoe mix (Jeffrey pine and white fir), with an initial carbon content of 49.02%. According to them, only 30 min were needed to increase the carbon content to 70.06 ± 0.13% at 255 °C. A further increase in reaction time, however, could not lead to a significant change in the carbon content (71.89% at 60 min). As shown in Table 2, in the present study the carbon content at 270 °C with 6 h treatment (72.53–75.27%) differs marginally from the content at 230 °C, and 6 h treatment (68.07–69.94%). According to literature as well as the present study confirm that HTC or thermal degradation of MCC requires temperature around 220–255 °C (Sevilla and Fuertes, 2009).

The curve of the carbonization (Fig. 2) shows that the conversion of MCC to a carbon-rich material occurs asymptotically, whereas the corresponding pressure increases quadratic manner. Increasing the temperature from 190 to 230 °C, results in a pressure gain of 1.7 MPa, while it is 2.9 MPa when temperature increases from 230 to 270 °C. This increase in pressure or temperature does not lead to a proportional increase of the carbon content. At pH below 7, the carbon content is between 42.52–55.02% (at 190 °C) and 67.08–69.45% (at 230 °C). The corresponding increase of the carbon content varies from 24.43% to 24.56% (at $\Delta T = 40$ °C). The same increase in temperature from 230 to 270 °C (carbon content of 71.16–75.27) only causes an increase in the carbon content of 4.08–5.82% (see Table 2). This corresponds to an average pressure of 2.6 MPa (230 °C), and 5.6 MPa (270 °C) (cf. Fig. 2). This shows that for the HTC, an optimum range of temperature is required. As the applied pressure is the most sensitive cost parameter in plants, from the perspective of economic efficiency, there is a demand to minimize the pressure as well as the reaction time. This choice of mild process conditions are supported by its positive yield effects: The higher the temperature and the higher the process pressure the lower is the char yield (Fig. 2). At 230 and 270 °C (each 6 h) the char yield were found at 47.30% and 44.70%, respectively (dry mass basis). The heating values (HV) of pristine and treated MCC at 6 h are shown in Table 2. As already mentioned by Boie (1953), the influence of temperature on the heating value is even of greater importance for the rationalization and modeling of thermal conversion of biomass. The higher the heating value of the char, the better will be the fuel. The hydrothermal treatment of MCC at 190 °C does not increase the heating value. In contrast to 190 °C, the treatment at 230 °C leads to a significant increase of heating value, which can be explained by the increase of the carbon content and the reduction of oxygen content in the hydrochar. The heating value of MCC treated at 230 °C (2–10 h) is 25 ± 1.5 MJ/kg comparing with the value at 270 °C (2–10 h), which is 26.00 ± 0.5 MJ/kg, indicating that it will be useful to perform the HTC process at mild temperatures ⩽230 °C. Which might solve the problem of high pressure requirement.

3.3. Behavior and effect of pH

In order to explain the decrease of pH, the liquid phases were analysed for determining the yield of formed carbon acids during the HTC process. The higher the HTC temperature, the higher the concentration of acetic and propionic acids in the liquid, while the concentrations of butyl acid, iso butyl acid, valeric acid and iso valeric acid were consistently less than 0.02 g/l (Table 2). Stemann shows that the concentration of acetic acid in the liquid phase is particular high (Stemann et al., 2013). During the trials, it was observed that the final pH remains almost constant at about 2.6 independently of process temperatures (190, 230, 270 °C), reaction times (2, 6, 10 h), and initial pH (cf. Table 2). This is due to the hydrolysis, which proceeds very quickly at high temperature. Only at 190 °C (and 2 h treatment or initial pH 7), the final pH level was found at a slightly higher (3.2). This agrees with the HTC results of Hoekman et al. (2011), showing that the variation of temperature and reaction time has little effect on the pH level. To identify the duration of experiment until the pH value remains constant, additional trials are necessary. The carbon concentration at trial number CE-05 (230 °C, 2 h, pH = 3) was 68.56% and significantly higher in comparison with the result at CE-08 (230 °C, 2 h, pH = 7), where the carbon content was 63.77%. Comparing the test number CE-02 (230 °C, 10 h, pH = 3) and CE-07 (230 °C, 10 h, pH = 7), a carbon content of respectively 69.45% and 68.40% was observed. At process conditions CE-04 (270 °C, 6 h, pH = 3), the carbon concentration was 75.27% in comparison with 72.53% at CE-06 (270 °C, 6 h, pH = 7). The observations suggest about two possible scenario regarding the effect of pH on HTC of MCC.

Hypothesis 1. The lower the reaction time, the higher the effect of lower pH level on the carbonization process (cf. sample CE-05/CE-08, where the time was 2 h). The same results were observed by runs CE-04 and CE-06 at a reaction time of 6 h. At process temperatures below 270 °C and reaction times less than 6 h, the pH level of the fed materials (MCC and water) should be as low as possible in order to obtain a carbon content of about 70%.

Hypothesis 2. At higher reaction times, the effect of the pH value decreases (cf. test run CE-02 and CE-07). At a time of 10 h, the carbon content remains similar, suggesting that HTC is independent of temperature and pH level. A reaction time of at least 10 h is required in order to ensure a higher carbon content and thus a higher degree of carbonization.

It can be concluded that altogether temperature, pH level and reaction time are important influence factors for hydrothermal carbonization. Comparing the results of the present study with those from Hoeckman et al. (2011), it can be noticed that at temperatures between 230 and 275 °C, MCC and lignocellulosic biomass carbonize similarly. For hydrothermal carbonization of MCC, a minimum of pressure is required, which happens at a temperature beyond 200 °C.

3.4. Results of the spectroscopic analyzes

3.4.1. Chemical shifts by NMR technique

HTC has a pronounced effect on the structure of hydrochar at different temperatures (Fig. S2). Whereas the ^{13}C CP/MAS spectrum of MCC treated at 190 °C is similar to that of cellulose upon higher temperatures (230 °C) the line shape changes completely. This is in line with results by Titirici et al. (2011), showing that at temperatures under 200 °C, MCC resist to hydrothermal treatment. Main resonances appear in the aromatic range (sp^2 hybridized carbon) around 120 ppm and in the aliphatic range around 14–75 ppm (sp^3 carbon). In addition, few carboxylated species are found as well at approx. 177 ppm and C=O motives around 210 ppm. Even though the CP/MAS measurement was not quantitatively analyzed, it appears that an increasing number of aromatic species are formed relative to the aliphatic sites in MCC treated at 270 °C. In addition, the increase of compounds found at 127 ppm and 151 ppm are the indications of further increase of aromatics, alkenes, and alkines relative to heteroaromatic compounds. The presence of graphite-like structures cannot be ruled out, but no probe detuning (even in the ^{1}H channel) was observed due to high conductivity of such phases. Hence, graphite-like structures do no play an important role in the investigated samples. The observed loss in oxygen through hydrothermal carbonization at 230 °C (final value, O = 26.03–27.70 AFDW%) compared to 270 °C (21.92–24.68 AFDW%) shows that aromatization proceeds further on upon temperature increase (cf. Table 2), indicating a higher stability of the hydrochars at 270 °C.

3.4.2. Vibrational spectroscopy

The ATR-FTIR spectrum of MCC processed at 190 °C resembles the typical spectrum of cellulose (Fig. S3) with strong vibrations including asymmetric stretching of C–O–C at 1159 cm^{-1} as well as skeletal vibration of the C–O stretching vibration at 1056 and 1029 cm^{-1} (Socrates, 2001; Uchimiya et al., 2011). In comparison with untreated cellulose, the MCC processed at 190 °C shows some decline of the broad band located at 3335–3284 cm^{-1}, which results from the –OH stretching vibrations indicating the onset of dehydration. MCC treated at higher temperatures exhibits complete different spectra, which is in-line with the ^{13}C CP/MAS spectra. Now, the typical C–O and C–O–C stretching vibrations and the intensity of hydroxyl peak at 3335–3284 cm^{-1} are strongly reduced giving rise to vibrations typical for aromatic compounds. However, the presence of C–H stretching vibration in the region 3000–2862 cm^{-1} is an indication of aliphatic structures. The appearance of new peaks at 1703, 1600, 863, 805, and 752 cm^{-1} suggests the formation of aromatic structures with C=C vibrations at 1600 cm^{-1}, an aromatic out of plane vibrations at 863–752 cm^{-1}. Furthermore, the formation of carbonyl, quinoide and/or carboxyl groups giving rise to the C=O vibrations can be deduced from the characteristic peak 1703 cm^{-1} (Socrates, 2001; Uchimiya et al., 2011). It should be noted that the C=C vibrations at about 1600 cm^{-1} are present in both spectra, however, with a higher absorbance from the MCC treated at 270 °C, indicating the increase of the aromatic structures and non-polar, and hydrophobic aromatic carbon surfaces. After the exposure of these surfaces to air over time, the carbon oxidizes, creating new oxygen-containing aromatic functional groups (–OH, –C=O, and –COOH), and making the surface polar again. These functional groups are the same as those found on soil organic matter and are critical for char–soil interaction (Brewer, 2012).

The spectral changes of MCC during hydrothermal treatment at 230 °C and 270 °C are an indication of dehydration and decarboxylation confirming the results of elemental analysis. However, in contrast to ^{13}C CP/MAS, here only minor differences between MCC treated at 230 °C and 270 °C were observed.

Raman spectroscopy provides an additional possibility on search for the presence of aromatic structures in hydrochar products. Only in MCC treated at 270 °C the typical G-band (1540 cm^{-1}), and D band (1380 cm^{-1}) can be observed (cf. Fig. S3). While the G band at 1587 cm^{-1} mainly involves the in-plane bond stretching motion of pairs of C sp^2 atoms in aromatic molecules and alkenes, the D band at 1360 cm^{-1} represents defect structures in highly ordered carbonaceous materials, and aromatics with not less than 6 rings in amorphous carbon (Tunistra and Koenig, 1970; Wu et al., 2009). For MCC treated at 190 °C both the D and G band are missing, and after 230 °C treatment, only a weak band in the region of the G band appears (Fig. S4). Consequently, formation of aromatic structures starts upon treatment with 230 °C, but only after 270 °C, a higher condensed structures being formed. This confirms the qualitative difference between MCC products formed at 230 °C and 270 °C observed by ^{13}C CP/MAS. It should be noted that Raman spectra here were recorded at 10 times lower laser power than in comparable studies (Tunistra and Koenig, 1970; Sevilla and Fuertes, 2009) in order to prevent burning of samples, which could result in the artificial formation of charred areas.

3.4.3. X-band ESR spectroscopy

X-band ESR spectroscopy detects the presence of paramagnetic centers in coal and charcoals providing information on both, nature and number of the observed species (Petrakis and Grandy, 1981; Cohen et al., 2006). The ESR spectra of all MCC based HTC products show one single peak without any fine or hyper-fine structure (Fig. S5). The *g* values at 190, 230, and 270 °C were determined about 2.0033, 2.0032, and 2.0028, indicating the presence of free organic radicals. Radicals form because of the thermal damage of carbon hydrogen bonds, when the unpaired electrons are stabilized by cyclic carbon π-system during the process of carbonization (Petrakis and Grandy, 1981; Cohen et al., 2006). Thermal treatment of organic material and charcoal increases the number of organic radicals up to temperatures about 550 °C when a maximum, whereas further heating is followed by a decline (Ingram et al., 1954). In the present study, an exponential increase of spin concentrations was observed, when the MCC was treated at up to 270 °C (exponential fit function: $y = 0.26{*}e^{(x/63)}$). The spin concentrations at temperatures 190, 230 and 270 °C were respectively determined about 1.2×10^{15}, 4.6×10^{16}, and 1.3×10^{17} g^{-1}. Aydas et al. (2010) attributed the increase of organic radicals during carbonization to an increase in the carbon content. However, according to the data in Table 2, the carbon concentration of HTC treated MCC does not increase exponentially in the investigated temperature range 190–270 °C. Hence, it must be rather the structural arrangement of the individual hydrochars, which allows for a more efficient stabilization of organic radicals inside the aromatic structures. The *g* values are highly sensitive to the chemical environment of the unpaired electrons in organic radicals (Paul et al., 2006). The observed shift towards smaller value suggests the presence of radicals in a more aromatic environment with increasing process temperature. The presence of higher radical numbers in structures with aromatic character further confirms the results of the NMR and Raman spectroscopic investigation. In contrast, ATR-FTIR spectra revealed only small differences between MCC treated at 230 and 270 °C. In case of possible inhomogeneities of the investigated MCC this would be most critical for ATR-FTIR where only small areas of the sample are probed, while NMR and ESR spectroscopic techniques gain information integrated over the complete sample volume. However, Raman spectroscopy, like ATR-FTIR mostly reports on sample properties in the sub-micron meter range. These observations facilitate the hypothesis of Sevilla and Fuertes (2009) who proposed the formation of core–shell particles during HTC of cellulose. The proposed solid particles consist of condensed benzene rings that form stable groups with oxygen in the core (i.e. *quinones*, *pyrones*) and more reactive/hydrophilic oxygen functionalities (i.e. hydroxyl, carbonyl, carboxylic) in the shell. Indeed, ^{13}C CP/MAS spectra revealed, next to a shift from heteroaromatic compounds to aromatics, the appearance of carboxylic groups for MCC processed at 270 °C. Both Raman- and ESR spectroscopy support a temperature dependent formation of condensed aromatic systems at 270 °C. Despite the small change in the carbon content about (6–10% from at 230 °C to 270 °C), the spectroscopic data clearly demonstrate that higher temperatures favor aromatization. If both the surface area, the pore structure, and high condensed carbon are required for the chars application, BET technique and spectroscopic methods such as NMR could give important informations about the chars physical structure and its chemical nature.

4. Conclusions

The hydrothermal carbonization of MCC has been studied, the solid and liquid phase analyzed. With regard to the physicochemical properties, the temperature range between 230 °C and 270 °C seems to be crucial for the HTC. The highest surface area (28.800 m^2/g) was generated at 230 °C, the carbon yield was between 63.77% and 69.45%, compared with the 270 °C char, where the yield and surface area were 75.20% and 9.003 m^2/g. ^{13}C CP/MAS results show a more stable hydrochar at 270 °C in contrast to FTIR, where minor differences between MCC treated at 230 °C and 270 °C were observed.

Acknowledgements

This research is supported by funds from the Bioenergy 2021 program delegated from the German Federal Ministry of Research and Education to Project Management Juelich (PtJ). Scanning electron microscope and surface analysis was carried out with technical support from the Dept. of Electron Microscopy (ZELMI) at Technische Universität Berlin. Additionally, the authors would like to thank E. Janiszewski, G. Rehde, A. Kohl and O. Haase for their support in analytical tasks.

Appendix A. Supplementary data

Supplementary data associated with this article can be found, in the online version, at http://dx.doi.org/10.1016/j.biortech.2013.09.129.

References

Aydas, C., Engin, B., Dönmez, E.O., Belli, O., 2010. The use of ESR technique for assessment of heating temperatures of archaeological lentil samples. Spectrochim. Acta A Mol. Biomol. Spectrosc. 75 (1), 466–473.

Becker, R., Dorgerloch, U., Helmis, M., Mumme, J., Diakité, M., Nehls, I., 2013. Hydrothermally carbonized plant material: patterns of volatile organic compounds detected by gas chromatography. Bioresour. Technol. 130, 621–628.

Bennett, A.E., Rienstra, C.M., Auger, M., Lakshmi, K.V., Griffin, R.G., 1995. Heteronuclear decoupling in rotation solids. J. Chem. Phys. 103, 6951–6958.

Boie, W., 1953. Fuel technology calculations. Energietechnik 3, 309–316.

Brewer, C.E., 2012. Biochar Characterization and Engineering. Graduate Theses and Dissertations. Paper 12284. Online: <http://www.lib.dr.iastate.edu/et>.

Cohen, O.I., Weiner, L., Boaretto, E., Mintz, G., Weiner, S., 2006. Modern and fossil charcoal, aspects of structure and diagenesis. J. Archaeol. Sci. 33, 428–439.

Day, D., Evans, R.J., Lee, J.W., Reicosky, D., 2005. Economical CO_2, SOx and NOx capture from fossil-fuel utilization with combined renewable hydrogen production and large scale carbon sequestration. Energy 30 (14), 2558–2579. In: Sohi, S., Loez, C.E., Krull, E., Bol, R. (Ed.), Biochar's Roles in Soil and Climate Change. A review of research needs, 2009. CSIRO Land and Water Science Report. Online, <http://www.csiro.au/files/files/poei.pdf>.

Funke, A., Ziegler, F., 2010. Hydrothermal carbonization of biomass: A summary and discussion of chemical mechanisms for process engineering. Biofuels. Bioprod. Bioref. 4, 160–177.

Goto, M., Obuchi, R., Hirose, T., Sasaki, T., Shibata, M., 2004. Hydrothermal conversion of municipal organic waste into resources. Bioresour. Technol. 93, 279–284.

Hoekman, S., Broch, A., Robbins, C., 2011. Hydrothermal carbonization (HTC) of lignocellulosic biomass. Energy Fuels 25, 1802–1810.

Ingram, D.J.E., Tapley, J.G., Jackson, R., Bond, R.L., Murnaghan, A.R., 1954. Paramagnetic resonance in carbonaceous solids. Nature 174, 797–798.

Lehmann, J., Joseph, S., 2009. Biochar for Environmental Management: Science and Technology. Earthscan, UK.

Libra, J.A., Ro, K.S., Kammann, A., Funke, A., Berge, N.D., Neubauer, Y., Titirici, M.M., Fuhner, A., Bens, O., Kern, J., Emmerich, K.H., (2011). Hydrothermal carbonization of biomass residuals: a comparative review of the chemistry, process, and applications of wet and dry pyrolysis. Biofuels 2 (1), 89–124.

Mumme, J., Eckervogt, L., Pielert, J., Diakité, M., Rupp, F., Kern, J., 2011. Hydrothermal carbonization of anaerobically digested maize silage. Bioresour. Technol. 102, 9255–9260.

Park, S., Baker, J.O., Himmel, M.E., Parilla, P.A., Johnson, D.K., 2010. Cellulose crystallinity index, measurement technique and their impact on interpreting cellulase performance. Biotechnol. Biofuels 3, 10. http://dx.doi.org/10.1186/1754-6834-3-10.

Paul, A., Stösser, R., Zehl, A., Zwirnmann, A.E., Vogt, R.D., Steinberg, C.E.W., 2006. Nature and abundance of organic radicals in natural organic matter, effect of sample pH and irradiation. Environ. Sci. Technol. 40, 5897–5903.

Petrakis, L., Grandy, D.W., 1981. Formation and behavior of coal free radicals in pyrolysis and liquefaction conditions. Nature 289, 476–477.

Reddy, G.B., 2010. Characterization and Application of Biochar. North Carolina A&T State University. Greensboro, NC, RFPPC. Annual Summit. Online, <http://www.fppcinc.org/pdf/2010-summit-speaker-presentations/GB-Ready-08-12-2010-Biochar-Ro.pdf>.

Reza, M.T., Yan, W., Uddin, M.H., Lynam, J.G., Hoekman, S.K., Coronella, C.J., Vásquez, R.V., 2013. Reaction kinetics of hydrothermal carbonization of loblolly pine. Bioresour. Technol. 139 (2013), 161–169.

Rouquerol, F., Rouquerol, I., Sing, K., 1999. Absorption by Powders and Porous Solid. Academic Press, London, UK.

Sandermann, W., Augustin, H., 1964. Chemical investigation on the thermal decomposition of woo – Part III. Chemical investigation on the course of decomposition. Holz als Roh-und Werkstoff 22 (10), 377–378.

Sevilla, M., Fuertes, A.B., 2009. The production of carbon materials by hydrothermal carbonization of cellulose. Carbon 47, 2281–2289.

Socrates, G., 2001. Infrared and Raman Characteristic Group Frequencies, Tables and Charts. John Wiley & Sons Ltd, Chichester, England, pp. 94–167.

Stemann, J., Putschew, A., Ziegler, F., 2013. Hydrothermal carbonization. Process water characterization and effects of water recirculation. Bioresour. Technol. 143, 139–146.

Titirici, M.M., Antonietti, M., Baccile, N., 2008. Hydrothermal carbon from biomass: a comparison of the local structure from poly- to monosaccharides and pentoses/hexoses. Green Chem. 10, 1204–1212.

Titirici, M.M., Falco, C., Baccile, N., 2011. Morphological and structural differences between glucose, cellulose and lignocellulosic biomass derived hydrothermal carbons. Green Chem. 13, 3273–3281.

Tunistra, F., Koenig, J.L., 1970. Raman spectra of graphite. J. Phys. Chem. 53, 1126–1130.

Uchimiya, M., Wartelle, L.H., Klasson, K.T., Fortier, C.A., Lima, I.M., 2011. Influence of pyrolysis temperature on biochar property and function as a heavy metal sorbent in soil. J. Agric. Food Chem. 59, 2501–2510.

Wang, L., Guo, Y., Zou, B., Rong, C., Ma, X., Q, Y., Li, Y., Wang, Z., 2011. High surface area porous carbon prepared from hydrochars by phosphoric acid activation. Bioresour. Technol. 102 (2), 1947–1950.

Weiner, B., Baskyr, I., Poerschmann, J., Kopinke, F.D., 2013. Potential of the hydrothermal carbonization process for the degradation of organic pollutants. Chemosphere 92, 674–680.

Wu, H., Yip, K., Tian, F., Xie, Z., Li, C.Z., 2009. Evolution of char structures during the steam gasification of biochars produced from pyrolysis of various mallee biomass components. Ind. Eng. Chem. Res. 48, 10431–10438.

Yordanov, N.D., Christova, A., 1997. Quantitative spectrophotometric and EPR-determination of 1,1-diphenyl-2-picryl-hydrazyl (DPPH). Fresenius' J. Anal. Chem. 358, 610–613.